*PRODUCTION ENGINEERING ARCHIVES 2022, 28(2), 157-163*

**PRODUCTION ENGINEERING ARCHIVES**

ISSN 2353-5156 (print)
ISSN 2353-7779 (online)

Exist since 4th quarter 2013
Available online at https://pea-journal.eu

# Surface Roughness Reduction in A Fused Filament Fabrication (FFF) Process using Central Composite Design Method

**Karin Kandananond**[1]

[1] Valaya Alongkorn Rajabhat University, 1 Moo 20, Paholyothin Rd., Pathum Thani, Thailand
Correspondence: karin@vru.ac.th

**Article history**
Received 15.07.2021
Accepted 27.11.2021
Available online 23.05.2022

**Keywords**
Average surface roughness
Central composite design
Fused filament fabrication

**Abstract**

The objective of this study is to optimize the fabrication factors of a consumer-grade fused filament fabrication (FFF) system. The input factors were nozzle temperature, bed temperature, printing speed, and layer thickness. The optimization aims to minimize average surface roughness (Ra) indicating the surface quality of benchmarks. In this study, Ra was measured at two positions, the bottom and top surface of benchmarks. For the fabrication, the material used was the Polylactic acid (PLA) filament. A response surface method (RSM), central composite design (CCD), was utilized to carry out the optimization. The analysis of variance (ANOVA) was calculated to explore the significant factors, interactions, quadratic effect, and lack of fit, while the regression analysis was performed to determine the prediction equation of Ra. The model adequacy checking was conducted to check whether the residual assumption still held. The total number of thirty benchmarks was fabricated and measured using a surface roughness tester. For the bottom surface, the analysis results indicated that there was the main effect from only one factor, printing speed. However, for the top surface, the ANOVA signified an interaction between the printing speed and layer thickness. The optimal setting of these factors was also recommended, while the empirical models of Ra at both surface positions were also presented. Finally, an extra benchmark was fabricated to validate the empirical model.

DOI: 10.30657/pea.2022.28.18 JEL: L69, M11

## 1. Introduction

One of the rapid prototyping (RP) techniques is the fused deposition modelling (FDM) or fused filament fabrication (FFF) method. Due to the FFF method, three-dimensional (3D) models were produced by depositing the melted material on the bed layer by layer to create the models' profile. Recently, the popularity of FFF seems to have increased significantly. One of the main reasons is the price of FFF systems which is currently affordable. As a result, there are many FFF system manufacturers which offer the customer-grade 3D printers. The main material of the FFF method is the polymer filaments, and Acrylonitrile butadiene styrene (ABS) is widely used because of its mechanical properties. Anyway, Polylactic acid (PLA) is another material that lately gained popularity because it is organically disposable and environmentally friendly. However, many properties of PLA are different from those of ABS; therefore, the insight understanding of PLA properties, and the characterization of FFF systems are important to enhance fabrication performance.

Regarding FFF process, a number of studies were conducted to determine the effect of different factors on surface quality. Armillotta (2006) studied the surface quality of different benchmarks manufactured on FDM system. The effect of surface patterns, different benchmark sizes, and aspect sizes was inspected to optimize the surface quality. Pandey and Reddy (2007) proposed the idea of improving the surface quality of finished parts fabricated by FDM system. The manufacturing technique used was the integration of lathe machine with FDM. The characterization of hybrid-FDM system led to the minimization of the parts' average surface roughness. Ahn et al. (2009) developed the expression of average surface roughness in the form of surface angles based on the empirical data. Turner and Gold (2015) reviewed studies regarding FDM processes. The responses were dimensional accuracy, resolution, and surface roughness. The important conclusion was that layer thickness had a significant impact on the value of surface roughness. Rahmati and Vahabli (2015) indicated that the slicing process and the tessellation of CAD models were the most important factor affecting surface quality. They also determined the accurate model to predict surface roughness by adjusting parameters based on the minimum average percentage error (MAPE) obtained in each setting condition. Li et al. (2017) carried out a comprehensive study on the effect of manufacturing techniques, namely Polyjet, FDM, and stereolithography (SLA), and types of materials, PLA, ABS, resin, Veroclear, and digital material. Other studied factors were layer thickness and infill density, while the response was surface roughness. Dewey and Ulutan (2017) utilized laser polishing technique to improve the quality of surface finish. The test parts were fabricated by FDM method, and the type of materials used was PLA. The results showed that average surface roughness was uniformed and fluctuated in a narrow range. Chohan and Singh (2017) studied the pre-and post-processing methods affecting the surface characteristics of test specimens. Input parameters were air gap, contour width, raster angle, raster width, and layer thickness for the pre-processing technique, while an output was surface roughness. Kim et al. (2018) performed a study on the surface roughness of FDM-fabricated parts. The effect of two types of parameters, fabrication (distance between nozzle and substrate, inflow speed of filament, and moving speed of heating nozzle) and extrusion (thickness, width, and the shape of cross section area), on surface roughness were experimentally analyzed.

Pérez et al. (2018) assessed the performance of FDM on test samples made of PLA filament. The study results indicated that layer height and wall thickness had an important effect on surface roughness. Another important finding was that printing path, printing speed, and temperature had no clear impact on surface quality. The statistical methods used were ANOVA, graphical representation, and non-parametric test. Tiwari and Kumar (2018) conducted a study to characterize an FDM system that was supplied with PLA filament. The analysis focused on the input factors (i.e., orientation, support, and gravity) and the dimensional accuracy of benchmarks. Taufik and Jain (2016) proposed a geometrical representation of workpieces with build edge profiles, and there were three types of profiles, perimeter-based, perimeter and raster-based, and raster-based. They also presented different models for determining surface roughness, theoretical models for raster-based edge and perimeter-based edge profiles and empirical model for the combination of both profiles (raster-based and perimeter-based). According to Medellin-Castillo and Zaragoza-Siqueiros (2019), layer thickness was not the only factor affecting surface roughness, the examples of other factors were types of materials, part and layer orientation, surface angle, distortion, shrinkage, warpage, and complex geometries.

Another aspect discussed in literature was the application of different experimental designs and machine learning methods to analyze the effect of input factors on surface roughness. Pandey et al. (2003) used fractional factorial method to analyze the effect of staircase effect on the surface roughness of RP parts. A study was carried out by Krolczyk et al. (2014) to analyze the surface roughness of workpieces manufactured by FDM method. The autocorrelation function and histogram of surface roughness were exploited for the analysis. The advantage of the analysis was the specific focus on the optimized conditions leading to achieve the lowest surface roughness. An RSM, Q-optimal design, was applied by Mohamed et al. (2016) to analyze and determine the mathematical model of surface roughness. The parameters of FDM system were layer thickness, air gap, raster angle, build orientation, road width, and a number of contours, and the surface roughness was designated as the response. Singh et al. (2017) utilized a design of experiment technique, Taguchi design, and the selected level design was a three-level design, L9. Benchmarks were fabricated using an FDM system, and the material used was ABS. The studied responses were the surface roughness and dimensional accuracy of benchmarks. To achieve the optimal FDM parameters, Peng et al. (2014) conducted a study regarding the effect of input parameters on the response. The inputs were line width compensation, extrusion velocity, filling velocity, and layer thickness. The outputs were dimensional error, warp deformation, and built time. They integrated the second-order response methodology with fuzzy inference to optimize the responses. Gurrala and Regalla (2014) selected CCD to optimize three parameters, build interior, horizontal build direction, and vertical build. There were two responses, evaluate strength and volumetric shrinkage, so two objective functions were determined. The responses were optimized by using genetic algorithm. For other methods, Vahabli and Rahmati (2016) used radial basis function neural network (RBFNN) method to predict the surface roughness of workpieces produced by FDM method. Wu et al. (2018) applied different methods, i.e., random forests (RFs), ridge regression (RR), least absolute shrinkage and selection operator (LASSO), and support vector regression (SVR), to train the predictive models for predicting surface roughness. Shirmohammadi et al. (2021) utilized hybrid ANN and particle swarm algorithm to optimize a 3D printing process by minimizing surface roughness.

Since surface roughness was an important characteristic of benchmarks fabricated by FFF system, it was chosen as the response of this study. For the system and material, the selected type of filament was PLA, widely used in the FFF process. A consumer-grade FFF unit was utilized as the fabrication system. The input factors were nozzle temperature, bed temperature, printing speed, and layer thickness. The response of this study was average surface roughness indicating the quality of the surface area. The focused surface area was not only the top position but also the bottom position, since the extruded filament was deposited on the print bed. Each layer of filament was compressed on the underneath layer. Moreover, the bottom surface directly contacted the printing bed. In contrast, the top surface was built upon the top layer of the filament. If the bottom or base layer had a good surface quality, it would provide a good support for the following layers and might influence the overall quality of a workpiece. Therefore, the roughness of bottom surface should also be minimized to achieve the best surface quality. Moreover, because the fabricated parts had more than one surface area, the analysis of influencing factors on surface roughness should be treated individually. In this study, these two surface areas, top and bottom, were measured and analyzed. Afterward, a response surface method, central composite design (CCD), was utilized to design the experiment. The effects of input parameters on the response were also characterized. These include main effect, interaction, and quadratic effect. Polynomial equations were modelled to predict the value average surface roughness. Eventually, the optimum settings of input factors were recommended to minimize average surface roughness at both surfaces.

## 2. Materials and Methods

The selected FFF system was the consumer-grade one that supported using PLA as the material. It also worked with the different types of materials, e.g., ABS. The system was an enclosed type and was pre-assembled from factory, and it came with an automatic bed-leveling. It was equipped with a single heating nozzle, and the maximum temperature was 240°C. The temperature of the heat plate was also adjusted up to 90°C. The smallest layer thickness of the filament extruded from the nozzle was 0.1 mm. The shape of benchmarks was rectangular prism that had flat surface on both sides (bottom and top). The selected line pattern of the benchmarks was rectilinear shape, and infill density was 10 percent. To prevent warping, print surface was covered by a printing build surface. The material used in this experiment was PLA, which was biodegradable. It was a white filament with the diameter of 1.75 mm, and it was packed in a spool. The dimensional accuracy was +/- 0.02 mm.

The solid model and a benchmark fabricated in this study are shown in Fig. 1. The benchmark dimension was 40 mm*100 mm* 4 mm. To fabricate workpiece, the solid model in the form of STL (Standard Tessellation Language) file was imported into a software package. Its profile was sliced into layers before being exported to a FFF system.

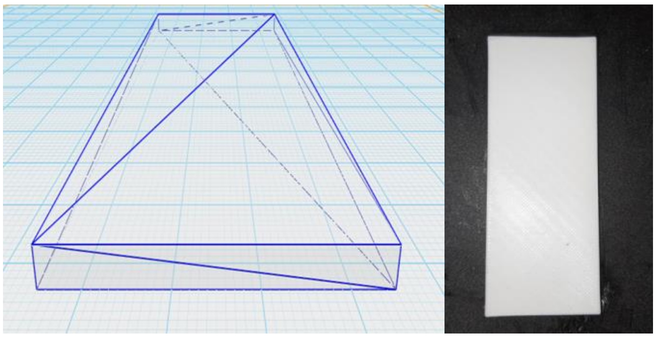

**Fig. 1.** Solid model and a benchmark

Since the surface roughness was used as the performance index of the workpiece quality, the average surface roughness was measured at the top and bottom surface. The analysis of the response was carried out separately by using an RSM. The ANOVA was generated to check the significance of each factor (main effect, interaction, and quadratic effect), overall model, block effect, and lack of fit. Afterwards, the empirical models for each response were determined, and the validation of the equation was also assessed. The statistical analysis was performed by using a design of experiment software, Design Expert.

### 2.1. Central Composite Design

RSM is a technique used to optimize the input factors to achieve the best response. The selected method in this study was CCD introduced by Box and Wilson (1951) and later Kiefer and Wolfowitz (1959). This design was able to determine the quadratic effect for the response. Another advantage of this design is the inclusion of the axial points, which depends on the value of α (distance from the center to the axial point). Basically, the value of α depends on the specific type of factorial designs used (full or fractional). For the full factorial design, the value of α is equal to α = (number of runs)$^{1/4}$. Therefore, if the factorial design is $2^k$, the value of α will equal $(2^k)^{1/4}$. Moreover, CCD has the capability to run the design in blocks. When there are two blocks in the design, these could be categorized as factorial and center point block and an axial point block. In addition, the application of CCD enables the checking capability of lack of fit. Finally, based on the analysis, regression equation is determined to predict the response variable. For example, if there are two significant factors with interaction and quadratic effects, the empirical model for independent variable ($x_1$ and $x_2$) is determined as follows:

$$\hat{y} = b_0 + b_1x_1 + b_2x_2 + b_{12}x_{12} + b_{11}x_1^2 + b_{22}x_2^2 \quad (1)$$

where $\hat{y}_i$ is the predicted value of a response, $b_0$ is the predicted constant coefficient, $b_1$ and $b_2$ are the predicted linear coefficient of $x_1$ and $x_2$, respectively, $b_{11}$ and $b_{22}$ are the predicted quadratic coefficient of $x_1$ and $x_2$, respectively, and $b_{12}$ is the predicted interaction coefficient.

In this study, four factors, printing speed (mm/sec), layer thickness (mm), nozzle temperature (°C), and bed temperature (°C), were selected as the inputs. Printing speed was the speed when each layer of a benchmark was printed or deposited on the printing bed. Nozzle temperature was the temperature that the extruder melts the filament before being solidified and deposited on the bed. Bed temperature was the temperature of a heated bed, while layer thickness is the thickness of the outer wall of a benchmark. Regarding the experiment, the levels of these factors were coded in five levels. The first two levels were -1 and +1 (factorial points), and another is 0 (center points). Moreover, there were additional levels (–α and +α) that were axial points. Since this design was $2^4$ factorial, the value of α was equal to $\alpha = (2^k)^{1/4} = (2^4)^{1/4} = 2$. As a result, the input factors and levels are listed in Table 1.

**Table 1.** Factors and the coded levels

| Factor | Coded Level | | | | |
|---|---|---|---|---|---|
| | -2 | -1 | 0 | +1 | +2 |
| A: Nozzle Temp. (ºC) | 215 | 220 | 225 | 230 | 235 |
| B: Bed Temperature (ºC) | 75 | 80 | 85 | 90 | 95 |
| C: Print. Speed (mm/sec) | 40 | 60 | 80 | 100 | 120 |
| D: Layer Thickness (mm) | 0.1 | 0.2 | 0.3 | 0.4 | 0.5 |

## 2.2. Measured Outcomes

Due to the experiment, there were a total number of thirty runs so thirty benchmarks were fabricated. There were two responses. The first response was the average surface roughness at the bottom position, Ra (bottom), and another was the average surface roughness at the top position, Ra (top). A surface roughness tester was used to measure the average surface roughness (Ra) of benchmarks. The surface tester used was equipped with the stylus, which travelled along a surface. The samples of fabricated benchmarks are depicted in Fig. 2. The numbers written on the benchmarks indicated the details regarding the treatment (first row = nozzle temperature, second-row = bed temperature, third row = printing speed, and fourth row = layer thickness).

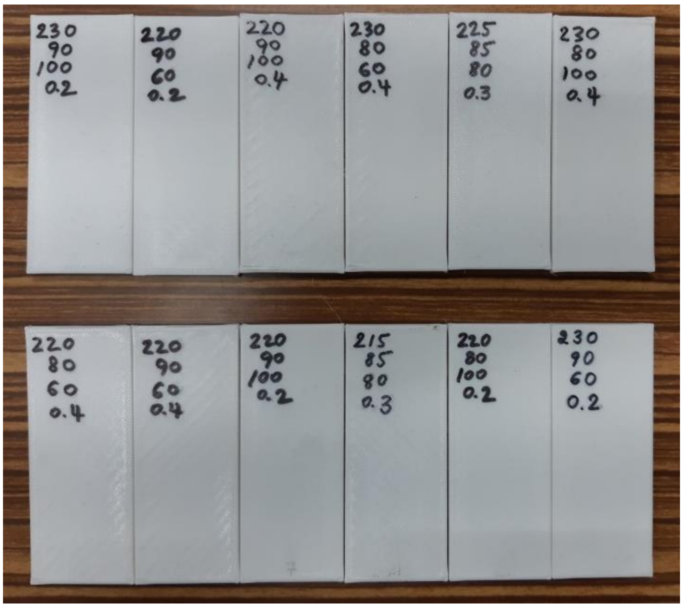


**Fig. 2.** Samples of fabricated benchmarks

The design matrix and the corresponded results are shown in Table 2. The selected design represented 4 factors with 30 runs composed of factorial design points, axial design points, and replicated center points. Moreover, there were two blocks (1st block: run 1-20 and 2nd block: run 21-30). The first block consisted of factorial design points and center points, and the second block was for the axial points.

**Table 2.** Design matrix and results

| Ord. | Nozzle temp (°C) | Bed temp (°C) | Print speed (mm/s) | Layer thick. (mm) | Ra (bottom) (µm) | Ra (top) (µm) |
|---|---|---|---|---|---|---|
| 1 | 220 | 80 | 60 | 0.2 | 5.01 | 3.62 |
| 2 | 230 | 80 | 60 | 0.2 | 7.14 | 3 |
| 3 | 220 | 90 | 60 | 0.2 | 6.51 | 2.08 |
| 4 | 230 | 90 | 60 | 0.2 | 7.11 | 3.68 |
| 5 | 220 | 80 | 100 | 0.2 | 22.7 | 2.67 |
| 6 | 230 | 80 | 100 | 0.2 | 17.32 | 2.35 |
| 7 | 220 | 90 | 100 | 0.2 | 18.34 | 2.02 |
| 8 | 230 | 90 | 100 | 0.2 | 21.3 | 2.63 |
| 9 | 220 | 80 | 60 | 0.4 | 10.79 | 12.2 |
| 10 | 230 | 80 | 60 | 0.4 | 8.62 | 10.62 |
| 11 | 220 | 90 | 60 | 0.4 | 7.31 | 11.55 |
| 12 | 230 | 90 | 60 | 0.4 | 5.48 | 10.07 |
| 13 | 220 | 80 | 100 | 0.4 | 23.3 | 14.81 |
| 14 | 230 | 80 | 100 | 0.4 | 20.1 | 14.59 |
| 15 | 220 | 90 | 100 | 0.4 | 18.76 | 16.56 |
| 16 | 230 | 90 | 100 | 0.4 | 18.55 | 16.89 |
| 17 | 225 | 85 | 80 | 0.3 | 10.05 | 6.62 |
| 18 | 225 | 85 | 80 | 0.3 | 11.86 | 6.74 |
| 19 | 225 | 85 | 80 | 0.3 | 10.41 | 6.28 |
| 20 | 225 | 85 | 80 | 0.3 | 12.95 | 6.69 |
| 21 | 215 | 85 | 80 | 0.3 | 12.22 | 6.55 |
| 22 | 235 | 85 | 80 | 0.3 | 10.92 | 4.95 |
| 23 | 225 | 75 | 80 | 0.3 | 8.63 | 11.05 |
| 24 | 225 | 95 | 80 | 0.3 | 16.28 | 7.29 |
| 25 | 225 | 85 | 40 | 0.3 | 5.19 | 8.68 |
| 26 | 225 | 85 | 120 | 0.3 | 17.7 | 8.48 |
| 27 | 225 | 85 | 80 | 0.1 | 12.12 | 3.7 |
| 28 | 225 | 85 | 80 | 0.5 | 14.28 | 13.05 |
| 29 | 225 | 85 | 80 | 0.3 | 13.07 | 9.69 |
| 30 | 225 | 85 | 80 | 0.3 | 12.01 | 6.54 |

# 3. Analysis

## 3.1. Bottom surface roughness

For bottom surface, the ANOVA in Table **3** shows that only printing speed (C) had a significant effect on Ra (bottom). Moreover, the analysis also indicated that the lack of fit was not significant, and there was no effect from blocks. Therefore, the proposed model was adequate enough to explain Ra (bottom).

**Table** 3**.** ANOVA for Ra (bottom)

| Source | SS | df | MS | F | p-value |
|---|---|---|---|---|---|
| Block | 5.87 | 1 | 5.87 | 3.94 | 0.12 |
| C-Print. Speed | 676.49 | 1 | 676.49 | 105.14 | < 0.0001 |
| Residual | 173.72 | 27 | 6.43 | | |
| Lack of Fit | 167.77 | 23 | 7.29 | 4.9 | 0.0664 |
| Pure Error | 5.95 | 4 | 1.49 | | |
| Cor Total | 856.09 | 29 | | | |

As a result, the prediction model for Ra (bottom) is determined as shown in (2).

$$Ra\ (bottom) = -8.525 + 0.2655 \cdot Printing\ speed \quad (2)$$

Another essential step towards the model building was the adequacy checking of residual. As a result, normal probability plot is presented in Fig. 3, depicting the externally studentized residual vs. percent of normal probability. The externally studentized residual was the difference between the observation and its predicted value divided by the estimated variance of the difference. The normal probability plot in Fig. 3 shows a straight-line pattern indicating there was no violation of residual assumption. Therefore, the residuals were normally distributed, so the proposed model was adequate to predict the surface roughness effectively.

The main effect plot is illustrated in Fig. 4 to quantify the effect of printing speed on Ra (bottom), when other factors were set at the average level as follows: nozzle temperature = 225°C, bed temperature = 85°C, layer thickness = 0.3 mm. According to Fig. 4, the best bottom surface quality was achieved when the printing speed was set at the lowest value (60 mm/sec). This result seemed to agree with the suggestion that surface quality was improved when printing speed was low (Yodo and Dey, 2021). Moreover, if the FFF was operated at higher printing speed, Ra (bottom) linearly increased until printing speed reached 100 mm/sec.

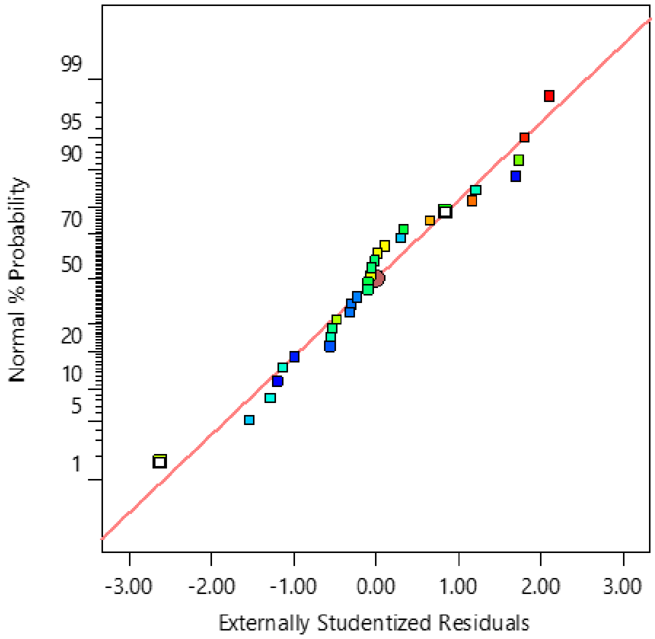


**Fig. 3.** Normal probability plot of residuals (bottom surface)

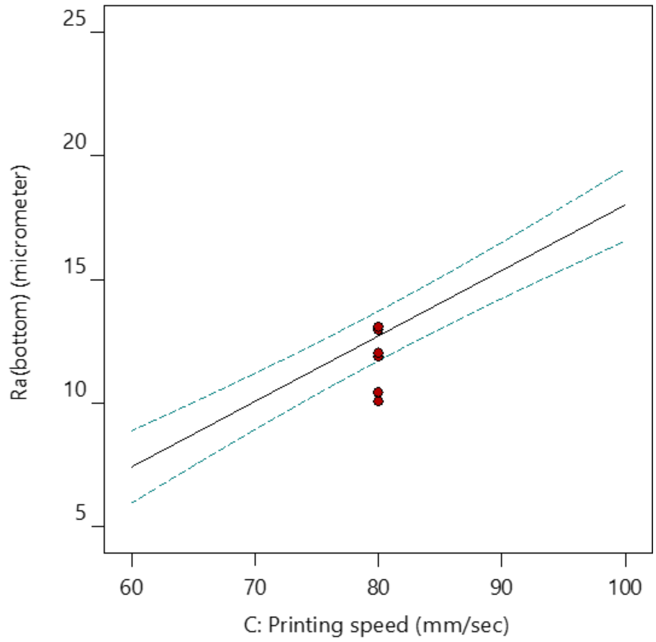


**Fig. 4.** Main effect plot of printing speed

## 3.2. Top surface roughness

Due to Ra (top), ANOVA in Table 4 shows that there were main effect (printing speed, C) and the interaction between printing speed (C) and layer thickness (D). There was no lack of fit and block effect. However, it was interesting to note that the square root transformation, $\sqrt{Ra + 0.5}$, was applied to the data so that the residual assumption still held. The regression equation for Ra (top) is shown in (3)

$$\begin{aligned} Sqrt\ (Ra\ (top) + 0.50) \\ &= 2.603 - 0.0265 \\ &\cdot Printing\ speed\ - 0.2556 \\ &\cdot Layer\ thickness + 0.1 \\ &\cdot Print.speed \cdot Layer\ thick \end{aligned} \tag{3}$$

**Table 4.** ANOVA for Ra (top)

| Source | SS | df | MS | F | p-value |
|---|---|---|---|---|---|
| Block | 0.1329 | 1 | 0.1329 | 3.544 | 0.13 |
| C-Print. Speed | 0.1182 | 1 | 0.1182 | 1.05 | 0.3146 |
| D-Layer. Thick. | 14.42 | 1 | 14.42 | 128.46 | < 0.0001 |
| CD | 0.6413 | 1 | 0.6413 | 5.71 | 0.0247 |
| Residual | 2.81 | 25 | 0.1123 | | |
| Lack of Fit | 2.66 | 21 | 0.1265 | 3.38 | 0.1228 |
| Pure Error | 0.1498 | 4 | 0.0375 | | |
| Cor Total | 18.12 | 29 | | | |

Normal probability plot is illustrated in Fig. 5. Since it showed a straight-line pattern, so it signified that the residuals from the prediction model were normally distributed. Therefore, there was no violation of residual assumption.

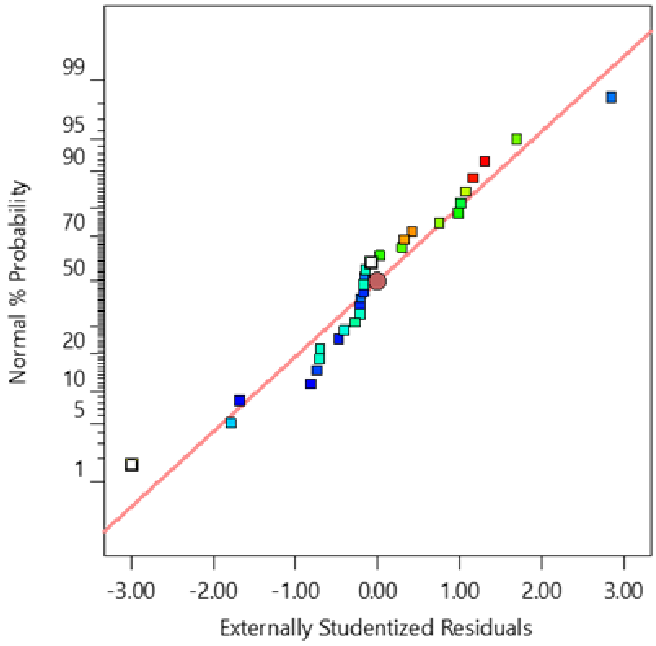


**Fig. 5.** Normal probability plot of residuals (top surface)

The contour plot of printing speed (C) and layer thickness (D) is presented in Fig. 6. The different contours of Ra (top), ranging from 4 to 12 µm, were plotted at the different levels of printing speed and layer thickness when the nozzle temperature and bed temperature were set at 225°C and 85°C, consecutively. For optimization, layer thickness should be set at the lowest level to minimize Ra (top). Due to the empirical results, if layer thickness was below 0.22 mm, printing speed would be between 70.8 and 100 mm/sec. On the other hand, when layer thickness was greater than 0.35 mm, printing speed should be set at the low level.

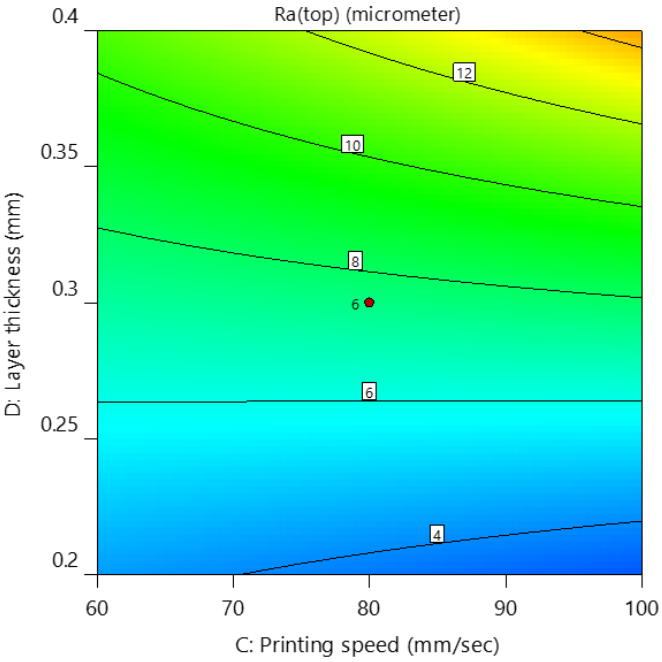


**Fig. 6.** Contour plot of printing speed and layer thickness

For the theoretical analysis of Ra (top), the obtained results were compared to a study by Taufik and Jain (2016) proposing the Ra computation model for different build edge profiles to predict the surface roughness of workpieces. One of this profile was the raster-based edge that had flat surface in the horizontal direction, and Ra depended on layer thickness ($l$) and edge profile deviation factor perpendicular-to-base-length direction ($k_h$). The deviation in the direction of profile height occurred because of neck-size formation. Therefore, the calculation of Ra by Taufik and Jain (2016) is shown in (4).

$$Ra = \frac{2000}{9\sqrt{3}}(l - 2k_h) \tag{4}$$

According to (4), the increment in layer thickness resulted in lower surface quality, and this relationship seemed to agree with the empirical study. However, another factor affecting the value of Ra was the deviation factor.

### 3.3. Validation

Another important step of the study was the validation of the prediction model. A benchmark was fabricated at the following conditions, nozzle temperature = 228°C, bed temperature = 88°C, printing speed = 90 mm/sec, and layer thickness = 0.25 mm, and it was utilized to validate the prediction model. As a result, Ra (bottom) and Ra (top) were measured and compared with the prediction results from the empirical models. The validation test from Table 5 shows the comparison of the responses from the observation and prediction. The results indicated that the values of observed Ra were not significantly different from the predict ones, so the prediction model was sufficient enough to estimate Ra (bottom) and Ra (top).

**Table 5.** Validation results

| Response | Obs. | S.D. | Predict |
|---|---|---|---|
| Ra (bottom) | 19.24 | 2.54 | 14.23 |
| Ra (top) | 7.59 | 1.62 | 4.6 |

## 4. Conclusions and discussions

The effect of four input factors, nozzle temperature, bed temperature, printing speed, and layer thickness, on the surface roughness, was investigated in this study. The CCD method was utilized to characterize the relationship between input factors and responses, Ra (bottom) and Ra (top). For Ra (bottom), surface roughness was minimized by setting printing speed at the lowest value. However, for Ra (top), there was an interaction between printing speed and layer thickness. The best surface quality of Ra (top) was achieved when workpieces were fabricated with the smallest layer thickness. The empirical models for both responses were also presented. Under some circumstances, although it was impossible to run a system at the optimal conditions (e.g., lowest printing speed), FFF operators were still able to decide what levels of printing speed and layer thickness should be. Therefore, the acceptable surface roughness was still achieved.

For discussion, two empirical models obtained in this study were derived to predict the values of Ra (bottom) and Ra (top). They were based on the empirical results and the CCD method. Therefore, since the obtained results were based on CCD, it is interesting to compare these results with the ones of another RSM, e.g., Box-Behnken. For four factors, Box-Behnken requires 27 runs which are fewer than those of CCD (30 runs). If the validation process shows that Box-Behnken is also an effective method, it will be another alternative choice of design to be considered.

Another point of discussion regarding the experiment is the effect of other factors on the surface roughness. This study focuses on the four input factors, nozzle temperature, bed temperature, printing speed, and layer thickness. However, it was noticed that, during the experiment, the bed surface was covered by a printing bed surface sheet to prevent warping and led to consistent print adhesion. It might be another factor affecting the surface quality. As a result, a further study should be conducted to quantify the effect of different printing build surfaces (e.g., blue tape, adhesive tape, glue stick) on the surface finish by adding them as a categorical factor.

## Reference

Ahn, D., Kweon, J.H., Kwon, S., Song, J., Lee, S., 2009. Representation of surface roughness in fused deposition modelling. Journal of Materials Processing Technology, 209(15–16), 5593-5600, DOI: 10.1016/j.jmatprotec.2009.05.016

Armillotta, A., 2006. Assessment of surface quality on textured FDM prototypes. Rapid Prototyping Journal, 12(1), 35-41, DOI: 10.1108/13552540610637255

Box, G.E.P., Wilson, K. B., 1951. On the experimental attainment of optimum conditions. Journal of the Royal Statistical Society. Series B, 13(1), 1-45.

Chohan, J.S., Singh, R., 2017. Pre and post processing techniques to improve surface characteristics of FDM parts: a state of art review and future applications. Rapid Prototyping Journal, 23(3), 495-513, DOI: 10.1108/RPJ-05-2015-0059

Dewey, M.P., Ulutan D., 2017. Development of laser polishing as an auxiliary post-process to improve surface quality in fused deposition modeling parts. Additive Manufacturing, 2, DOI: 10.1115/MSEC2017-3024

Gurrala, P.L., Regalla, S.P., 2014. Multi-objective optimisation of strength and volumetric shrinkage of FDM parts. Virtual and Physical Prototyping, 9(2), 127-138, DOI: 10.1080/17452759.2014.898851

Kiefer, J., Wolfowitz, J., 1959. Optimum designs in regression problems. Annals of Mathematical Statistics, 30, 271–294.

Kim, M.K., Lee, I.H., Kim, H.C., 2018. Effect of fabrication parameters on surface roughness of FDM parts. International Journal of Precision Engineering and Manufacturing, 19(1), 137–142, DOI: 10.1007/s12541-018-0016-0

Krolczyk, G., Raos, P., Legutko, S., 2014. Experimental Analysis of Surface Roughness and Surface Texture of Machined and Fused Deposition Modelled Parts. Tehnički vjesnik, 21(1).

Li, Y., Linke, B. S., Voet, H., Falk, B., Schmitt, R., Lam, M., 2017. Cost, sustainability and surface roughness quality – A comprehensive analysis of products made with personal 3D printers. CIRP Journal of Manufacturing Science and Technology, 16, 1-11, DOI: 10.1016/j.cirpj.2016.10.001

Medellin-Castillo, H.I., Zaragoza-Siqueiros, J., 2019. Design and manufacturing strategies for fused deposition modelling in additive manufacturing: a review. Chinese Journal of Mechanical Engineering, 32(53), DOI: 10.1186/s10033-019-0368-0

Mohamed, O.A., Masood, S.H., Bhowmik, J.L., 2016. Mathematical modeling and FDM process parameters optimisation using response surface methodology based on Q-optimal design. Applied Mathematical Modelling, 40(23-24), 10052-10073, DOI: 10.1016/j.apm.2016.06.055

Pandey, P.M., Reddy, N.V., Dhande, S.G., 2003. Improvement of surface finish by staircase machining in fused deposition modelling. Journal of Materials Processing Technology, 132(1–3), 323-331, DOI: 10.1016/S0924-0136(02)00953-6

Pandey, P.M., Reddy, N.V., 2007. Virtual hybrid-FDM system to enhance surface finish. Virtual and Physical Prototyping, 1(2), 101-116, DOI: 10.1080/17452750600763905

Peng, A., Xiao, X., Yue, R., 2014. Process parameter optimisation for fused deposition modeling using response surface methodology combined with fuzzy inference system. International Journal of Advanced Manufacturing Technology, 73 (1-4), 87-100, DOI: 10.1007/s00170-014-5796-5

Pérez, M., Medina-Sánchez, G., García-Collado, A., Gupta, M., Carou, D., 2018. Surface quality enhancement of fused deposition modeling (FDM) printed samples based on the selection of critical printing parameters. Materials, 11(8), 1382, DOI: 10.3390/ma11081382

Rahmati, S., Vahabli, E., 2015. Evaluation of analytical modeling for improvement of surface roughness of FDM test part using measurement results. International Journal of Advanced Manufacturing Technology, 79(5–8), 823–829, DOI: 10.1007/s00170-015-6879-7

Shirmohammadi, M., Goushchi, S.J., Keshtiban, P.M., 2021. Optimization of 3D printing process parameters to minimize surface roughness with hybrid artificial neural network model and particle swarm algorithm. Progress in Additive Manufacturing, 6, 199-215, DOI: 10.1007/s40964-021-00166-6

Singh, R., Singh, S., Singh, I. P., Fabbrocino, F., Fraternali, F., 2017. Investigation for surface finish improvement of FDM parts by vapor smoothing process. Composites Part B, 111, 228-234, DOI: 10.1016/j.compositesb.2016.11.062

Taufik, M., Jain, P., 2016. A study of build edge profile for prediction of surface roughness in fused deposition modelling. Journal of Manufacturing Science and Engineering, 138(6), DOI: 10.1115/1.4032193

Tiwari, K., Kumar, S., 2018. Analysis of the factors affecting the dimensional accuracy of 3D printed products. Materials Today, 5(9), 18674-18680, DOI: 10.1016/j.matpr.2018.06.213

Turner, B., Gold, S., 2015. A review of melt extrusion additive manufacturing processes: II. Materials, dimensional accuracy, and surface roughness. Rapid Prototyping Journal, 21(3), 250-261, DOI: 10.1108/RPJ-02-2013-0017

Vahabli, E., Rahmati, S., 2016. Application of an RBF neural network for FDM parts' surface roughness prediction for enhancing surface quality. International Journal of Precision Engineering and Manufacturing, 17, 1589–1603, DOI: 10.1007/s12541-016-0185-7

Wu, D., Wei, Y., Terpenny, J., 2018. Predictive modeling of surface roughness in fused deposition modeling using data fusion. International Journal of Production Research, 57(3), 3992-4006, DOI: 10.1080/00207543.2018.1505058

Yodo, N., Dey, A., 2021. Multi-objective optimization for FDM process parameters with evolutionary algorithms. Fused Deposition Modeling Based 3D Printing (Editors: Dave, H. K., Davim, J. P.), Springer International Publishing, Basel, Switzerland.


# 使用中心复合设计方法降低熔丝制造 (FFF) 工艺中的表面粗糙度


**關鍵詞**
平均表面粗糙度
中央复合设计
熔丝制造



**摘要**
本研究的目的是优化消费级熔丝制造（FFF）系统的制造因素。输入因素是喷嘴温度、床温、打印速度和层厚。优化旨在最小化表示基准表面质量的平均表面粗糙度 （Ra）。在这项研究中，Ra 在两个位置测量，即基准的底部和顶部表面。对于制造，使用的材料是聚乳酸 （PLA） 长丝。响应面法（RSM），中心复合设计（CCD），被用来进行优化。计算方差分析（ANOVA）以探索显着因素、交互作用、二次效应和失拟，而进行回归分析以确定Ra的预测方程。进行模型充分性检查以检查残差假设是否仍然成立。使用表面粗糙度测试仪制作和测量了总共三十个基准。对于底面，分析结果表明，主要影响因素只有一个，印刷速度。然而，对于顶面，ANOVA 表示打印速度和层厚度之间的相互作用。还推荐了这些因素的最佳设置，同时还提出了两个表面位置的 Ra 的经验模型。最后，制作了一个额外的基准来验证经验模型。